Optimizing acquisition and fitting conditions for ^{1}H MR spectroscopy investigations in global brain pathology

Maike Hoefemann[1,2], Victor Adalid[1], Roland Kreis[1]

[1]Depts. Radiology and Biomedical Research, University of Bern, Bern, Switzerland

[2]Graduate School for Cellular and Biomedical Sciences, University of Bern, Bern Switzerland

Corresponding author:

Prof. Dr. sc. nat. Roland Kreis, AMSM, University Bern, Erlachstrasse 9a, CH-3012 Bern, roland.kreis@insel.ch

Abstract

Purpose: To optimize acquisition and fitting conditions for non-focal disease in terms of voxel size and use of individual coil element data. Increasing the voxel size yields higher signal-to-noise, but leads to larger linewidths and more artifacts. Several ways to improve spectral quality for large voxels are to be exploited and the optimal use of individual coil signals investigated.

Methods: 10 human subjects were measured at 3T using a 64-channel receive head coil with a semi-LASER localization sequence under optimized and deliberately misset field homogeneity. 8 different voxel sizes (8 to 99 cm^3) were probed. Spectra were fitted either as weighted sums of the individual coil elements or simultaneously without summation. 18 metabolites were included in the fit model that also included the lineshapes from all coil elements as reflected in water reference data. Fitting errors for creatine, myo-inositol and glutamate are reported as representative parameters to judge optimal acquisition and evaluation conditions.

Results: Minimal Cramer-Rao lower bounds and thus optimal acquisition conditions were found for a voxel size of about 70 cm^3 for the representative upfield metabolites. Spectral quality in terms of lineshape and artifact appearance was determined to differ substantially between coil elements. Simultaneous fitting of spectra from individual coil elements instead of traditional fitting of a weighted sum spectrum lowered Cramer-Rao lower bounds by up to 17% for large voxel sizes.

Conclusion: The optimal voxel size for best precision in determined metabolite content is surprisingly large. Such an acquisition condition is most relevant for detection of low-concentration metabolites, like NAD^+ or phenylalanine, but also for longitudinal studies where very small alterations in metabolite content are targeted. In addition, simultaneous fitting of single channel spectra enforcing lineshape and coil sensitivity information proved to be superior to traditional signal combination with subsequent fitting.

Key words

spectral quality; signal acquisition; artifacts; lineshape; modeling

List of Abbreviations

Cr- creatine

CRLB – Cramer Rao Lower Bounds

CSI – chemical shift imaging

GABA - γ-aminobutyric-acid

Gln - glutamine

Glu – glutamate

Gly - glycine

GSH - gluthathione

HLSVD - Hankel-Lanczos Singular Value Decomposition

mI – myo-Inositol

NAA - N-acetylaspartate

ROI – region of interest

SNR – signal to noise

TD – time domain

VS – voxel Size

1. Introduction

In clinical Magnetic Resonance Spectroscopy (MRS) with its inherently low Signal to Noise Ratio (SNR) and strict restraints in acquisition time, the optimal choice of acquisition parameters is of great importance. For non-focal disease, the SNR, which is one of the crucial determinants for the precision and stability of the derived metabolite data, can be maximized by the use of a large voxel size (VS) which could, in the extreme case, be the maximum cuboid voxel possible to inscribe in supraventricular brain (close to 100 cm^3 for large heads). One example for the need of a large VS is the detection of the low-concentration metabolite phenylalanine in patients suffering from phenylketonuria, where a measurement over a large region of the brain is necessary[1]. Another recent example is the detection of NAD^+, which also depends on optimal signal from a large voxel[2]. However, increasing the VS may also lead to increased linewidths, reducing the spectral resolution and hence compromising the spectral quality. In addition, increasing the region of interest (ROI) also places the edges of the voxel closer to areas outside the brain, favoring the occurrence of outer-volume artifacts such as spurious lipids[3–5]. Therefore, a compromise between these contributors to spectral quality is necessary.

The optimal VS has been investigated for chemical shift imaging (CSI) by Hanson et al.[6], who investigated the effect of VS on extrapolated pure gray and white matter contents and stated that a relatively large VS can be used with only minor increase in estimation errors. In this context, it should be noted that post-acquisition summation of spectra from individual pixels from a CSI acquisition yields much lower SNR than the single voxel acquisition of that region. This can readily be understood realizing that the SNR for the spectra of each CSI-pixel roughly corresponds to the SNR of the same ROIs targeted by a single voxel (neglecting intravoxel dephasing) but that increasing this region of interest in SV MRS linearly increases the SNR with the targeted volume (no increase in noise) while adding spectra from neighboring pixels in CSI will increase the SNR only with the square root of the number of pixels because of the additive noise. Therefore, CSI is not an option for best SNR per measurement time. For single voxel spectroscopy, Fleysher et al.[3] showed in a theoretical set-up that for any B_0 field strength there is an optimized VS, linking the spectral and spatial resolutions, which can be calculated in an experimental procedure. However, no definite value for optimal VS was defined. Therefore, an experimental study resulting in practical VS recommendations for a given B_0 is of interest.

This can be done by using Cramer Rao Lower Bounds (CRLB) as the quality indicator for different VS. CRLB have proven to provide a useful tool for evaluating fitting precision in MRS, as they constitute an estimate of the lowest possible variance for the fitted parameters. In addition, they also offer insight into the beneficial effect of prior knowledge constraints[7,8]. This study uses CRLB as an

indicator for optimal acquisition conditions reflected in lowest fitting uncertainty, to investigate the optimal VS as a compromise of the different aspects of spectral quality.

In fitting techniques that include an analytic description of the lineshape, metabolite signal decay is described by a Voigt model that contains both an exponential and a Gaussian decay to cope with the natural T_2 decay of the metabolite signals as well as the linebroadening due to residual B_0 field inhomogeneity after shimming. This approach relies on an approximately random Gaussian distribution of the bias field, which may not be realistic, especially when it comes to larger VS where macroscopic inhomogeneities may lead to field distributions that cannot be corrected properly with second order shims. Therefore, an arbitrary lineshape can be modeled during the fit[9,10] or a reference lineshape can be derived from the non-suppressed water signal, which suffers from the same distortions as the metabolite signals in the water-suppressed spectrum, to improve the suitability of the fitting model[11–16]. The use of such a reference lineshape seems thus appropriate when optimizing the acquisition settings for larger ROIs and will be investigated in this study.

Modern multichannel receive arrays offer the possibility to gain spatially distinct views of the overall signal. Spatially distinct views of MRS signals have been used for speeding up chemical shift imaging scans (e.g. based on SENSE[17]) but have not been explored much to improve single voxel spectra. The only aspect that has been investigated is the optimal combination of the signals from individual channels to optimize the SNR of the summed spectrum, where different weights have been suggested, either based on signal intensity, SNR, signal intensity per square of the noise[18–23] or considering correlated noise[24]. However besides SNR, spectral quality also depends on linewidth or presence of artifacts, which may differ for the signals seen from individual spatially distinct coil elements. This aspect has been considered for the combination of repeated measurements to an averaged spectrum where alignment in frequency has been introduced and reliability of the individual signals to reduce signal artifacts in the resulting signal[25] has been explored. Here, we explore whether combination of simultaneously recorded signals from different coil elements can also be scrutinized to improve these aspects of spectral quality. In particular, this was examined for an ROI placed above the ventricles in a brain region that offers sufficient space for extremely large VS and a good shim. To simulate less optimal scanning conditions all scans were repeated with manipulated shimming parameters.

In summary, this contribution shows several approaches to improve spectral quality for large VS, considering the optimal VS as a compromise of SNR and spectral resolution as well as artifact appearance. In addition, the optimal use of individual coil signals is investigated, taking into account

differences in spectral quality and taking advantage of the non-water-suppressed signal as reference for all coil elements.

2. Methods

2.1 Data acquisition

All data was acquired on a 3T MR scanner (Prisma, Siemens, Erlangen, Germany) using a 64-channel head coil, with 44 channels in use (excluding the channels in the neck region) and a semi-LASER localization sequence[26] with the manufacturers second order shimming routine (option "brain", a fieldmap method with finer resolution than the old default method) and outer-volume suppression in the direction of the non-adiabatic excitation pulse (not used for the water reference scans). To simulate limited field homogeneity all measurements were repeated with intentionally misset shimming parameters, arbitrarily manipulating the X^2Y^2 shim current with a constant offset.

In vivo data was collected from 10 healthy subjects (28 ± 12 years of age). 8 different voxels, placed above the ventricles (Figure 1a) with sizes ranging from 8 to 99 cm^3 (8; 32; 48; 60; 75; 85; 88; 99 cm^3) and with a constant thickness of 2 cm in head/feet-direction (localized by the non-adiabatic RF pulse) and was measured for each subject with the acquisition parameters of TE = 51 ms (minimum TE for the specific hyperbolic secant RF pulses and power available) and TR = 3000 ms. VAPOR water suppression was used with a bandwidth of 135 Hz and 32 acquisitions were averaged for each measurement. Additionally, a single-shot measurement of the non-suppressed water signal with the same gradients played out as for the water-suppressed scans was recorded for each case. The transmit frequency was set to 3 ppm for the water-suppressed scans and to the water resonance at 4.7 ppm for the reference acquisition. Spectral BW was 2000 Hz and 2048 points were acquired.

2.2 Fitting procedure

Fitting of all spectra as well as noise estimation was done with the fitting tool “FiTAID”[27], which uses Voigt lineshapes for modeling the spectral responses and includes the option of reference-lineshape enhanced fitting[16], where the lineshape obtained from unsuppressed water is applied to the model spectra to extend the basic Voigt lineshape. Prior to including the water lineshape into the model, the major amount of its T_2 decay is removed as this varies from the metabolite signals. Fitting parameters include Lorentzian and Gaussian linewidth, frequency offset, zero-order phase and area. Frequency offset was enforced to be identical for all metabolites. In case of lineshape integration, negative Lorentzian values were allowed to account for insufficient water T_2 decay removal.

Prior to the fitting process the residual water was suppressed using Hankel-Lanczos Singular Value Decomposition (HLSVD) filtering in JMRUI[28]. A basis set of 18 metabolites (Aspartate; Creatine (Cr); Ethanolamine; γ-aminobutyric-acid (GABA); Glucose; Glutamine (Gln); Glutamate (Glu); Glycine (Gly); Glycerophosphorylcholine; Glutathione (GSH); Lactate; myo-Inositol (mI); N-acetylaspartate (NAA); N-acetylaspartylglutamate; Phosphocholine; Phosphorylethanolamine; scyllo-Inositol; Taurine) was simulated in VeSPA[29], using an ideal (i.e. using perfect 180° rotations in spin density matrix calculations) PRESS experiment. Since J-evolution during TE is partially suppressed with a semi-LASER sequence (reduced J-evolution in times under RF irradiation), the best-matching echo time for the simulation with an ideal PRESS sequence was optimized by comparing in vitro spectra with spectra simulated for different TEs, as previously suggested[30]. An echo time of 28 ms was chosen for the simulations since this was found to best represent the J-evolution pattern of our semiLASER sequence with TE 51 ms (see supplemental Figure S1 for illustration). A predefined model of the macromolecular baseline was added to the fit, which was allowed to adapt its overall area during the fitting process. Frequency offset and phase was linked to the metabolites. The fitting range was set to 0 to 4 ppm. A single Voigt line was added at 4.7 ppm to correct for potential baseline modifications from residual water removal.

To simplify the fitting process, all metabolites were prescribed to have the same T_2, such that the Lorentzian linewidth was assumed to be identical for all metabolites. Lorentzian linewidth and therefore T_2 was allowed to adjust for each spectrum. Phase, frequency offset and Gaussian linewidth was assumed not to vary between the metabolites and were therefore linked to identical values.

Evaluation of the benefit of using individual coil channel spectra was performed for all subjects on 5 of the 8 VS (8, 48, 60, 75 and 88 cm^3), each for optimized and misset shim. With the 2D fitting process of FiTAID, it is possible to simultaneously fit all coil elements instead of using the average over all elements. Implementing the water signal as reference also introduces the measured water amplitude ratio of signal intensities between the elements, since the unscaled lineshape reference signal is multiplied with the signal model in time domain (TD). This approach also accommodates differences in center frequency seen for the individual coil elements, allowing a simultaneous fitting approach of all individual channel spectra. Given that the noise was very similar for all channels, the simultaneous fitting of the individual channel spectra is equivalent to water-SNR weighted averaging for the combination of the individual coil element data.

CRLB of the metabolite area as determined in FiTAID under consideration of the lineshape and common fit of coil elements were used to estimate the precision of the fit[8]. Results of three metabolites with representative patterns were chosen for detailed analysis: Cr, Glu and mI, where

both Glu and mI might be particularly sensitive to suboptimal shim because of their substantial overlap with other metabolite pattern (Gln, Gly, respectively). Interindividual scaling and, hence, calculation of absolute CRLB was based on the water resonance as reference.

2.3 Evaluation of SNR and metabolite linewidth

To untangle SNR and linewidth effects, a definition of SNR in TD was used. It was defined as the second point of the metabolite signal in TD[1] after filtering out the residual water peak using HLSVD[28], divided by two times the standard deviation of the noise in TD, which was evaluated at the last 500 points of the FID. Success of HLSVD filtering was checked by visual inspection in each case so that the SNR calculation was not affected by residual water.

$$SNR_{metab} = \frac{intensity_{metab,TD}}{2 * SD_{noise,TD}}$$

The overall metabolite linewidth (LW_{Voigt}) was calculated as a combination of the fitted parameters of the Lorentzian (LW_{Lor}) and Gaussian linewidth (LW_{Gau}) (from an analysis without reference lineshape in the model) [31].

$$LW_{Voigt} = 0.5346 * LW_{Lor} + \sqrt{0.2166 * {LW_{Lor}}^2 + {LW_{Gau}}^2}$$

2.4 Handling of individual coil elements

For combining the individual element signals to a summed spectrum, SNR weighting was chosen. As the noise was considered to be non-related and proved to be equal in mean amplitude (varied by 3% between channels only) for all elements, the intensity of the referenced non water-suppressed signal was used as a weighting factor. The signal intensity was estimated from the absolute value of the second point in TD (*iwref*). Apart from a scaling factor, the average spectrum obtained with this procedure equaled the average spectrum provided by the scanner.

$$Spectrum_{avg} = \frac{1}{iwref_{sum}} * \sum_{n=1}^{\substack{number\ of \\ coil\ elements}} iwref_n * spectrum_n$$

[1] The first point in the FID is not well suited because it is influenced by the receive filters of the scanner

$$iwref_{sum} = \sum_{n=1}^{\substack{number\ of \\ coil\ elements}} iwref_n$$

As the distribution of artifacts, e.g. from lipid signals, differs between the individual coil channels, we tried to exclude afflicted channels from the overall averaged spectrum to increase spectral quality. An automated method was developed, which finds those channels that show an extraordinarily high deviation from the average signal of all channels in any frequency range. A detailed description of the method can be found in the supplemental material (Text and Figure S2).

3. Results

3.1 Effect of voxel size on spectral quality

As expected, SNR and linewidth were both found to increase with VS. This dependence is illustrated qualitatively with representative spectra and quantitatively with cohort results, both in Figure 1b. Quite surprisingly, the linewidth remained well below 12.5 Hz even for the largest ROI for most subjects (9 of 10 cases with optimized shim, 6 of 10 for misset shim). While for the SNR the shim performance does not have any relevant impact (as expected for a TD-SNR) it is substantial for the linewidth. For the largest VS of 99 cm^3, the linewidth showed values of 8.5 ± 2.8 Hz for optimized shimming and 11.2 ± 3 Hz for misset second order shims.

3.2 Finding the optimal voxel size

Evaluation of the optimal VS was done primarily for the coil averaged spectra. CRLB for the three chosen representative metabolites are illustrated in Figure 2 as a function of VS. CRLB clearly decrease with increasing VS up to around 70 cm^3. Beyond, there seems to be a marginal benefit only, though no clear increase in CRLB is seen either, but it was noted that in some cases (particularly with some head motion) large outer-volume fat signals could contaminate the spectrum at VS > 75 cm^3. Using the lineshape information reduced the CRLB, especially when it comes to larger VS and poor shimming. For the large VS of 75 – 99 cm^3 the absolute decrease of CRLB due to lineshape information for Cr, Glu and mI was on average 0.0042 mmol/l, 0.0042 mmol/l and 0.0014 mmol/l for optimized shim, which is a relative decrease of 22.9%, 8% and 2.9%, respectively. For misset shim, the CRLB could be reduced by 0.0085 mmol/l, 0.0035 mmol/l and 0.0057 mmol/l or 32.5%, 18.8% and 8%, respectively. For a metabolite spectral pattern consisting of narrow features only (e.g. Cr) the relative increase in fitting precision from the known reference lineshape is much larger than for the broader patterns of e.g. mI and Glu. However in absolute terms, it is inverse because the CRLB for Cr are intrinsically very small for the large singlets of Cr.

3.3 Evaluation of signals from individual coil elements

3.3.1 Differences between individual coil elements

Figure 3 illustrates substantial differences between data from individual channels in the described quality aspects SNR, linewidth and in the appearance of lipid artifacts for the water-suppressed spectra in a single representative subject for three large VS with optimized shim. Some sample water lineshapes from the respective reference measurements revealed that apart from varying signal intensities there are also differences in frequency offset as well as in the general shape of the responses.

3.3.2 Fitting spectra from individual coil elements simultaneously

Fitting the spectra from all coil elements simultaneously instead of fitting the summed spectrum leads to smaller CRLB. The extent of the improvement in fit precision as function of VS is depicted in Figure 4 for the case that the lineshape information is enforced. The relative benefit from this extended fitting procedure increases with VS. For the largest evaluated VS (88 cm^3) CRLB decreased by 12-16% for the optimized shim case and similarly by 13-17% for a misset shim. For smaller ROIs, the decrease in CRLB was generally more expressed with misset shims (8-12%). For the smallest VS of 8 cm^3, the absolute decrease is larger compared to higher VS; however, the relative decrease is smaller (0.2 – 5% for optimized shim and 5-8% for misset shim).

3.3.3 Exclusion of coil elements to reduce artifacts

The procedure of excluding single coil elements was tested on all subjects for a VS of 88 cm^3. The number of excluded channels differed considerably between 0 and 31 out of the 44 channels. For most cases, no appreciable influence on the resulting averaged spectrum was found.

To test the method for less optimal conditions, e.g. due to a different type of localization sequence, an additional scan in a single subject was investigated with both the otherwise used semi-LASER and additionally the manufacturer's PRESS sequence. For the PRESS sequence no outer-volume-suppression was used. As expected, the spectral quality was lower with PRESS, especially regarding the amount of lipid artifacts and also the linewidth. Figure 5 shows the averaged spectra with and without use of the automated channel exclusion method. In this case, for semi-LASER no channels were flagged to be excluded, while for PRESS, a clear benefit of excluding channels with inferior spectral quality is apparent. Note that despite a signal loss of 22% this does not infer any appreciable loss in SNR as the noise also decreased with the exclusion of coil elements and there was concomitant improvement regarding artifacts and peak shape.

4. Discussion

The presented investigations are directed at finding optimal acquisition, processing and fitting conditions for the case of quantification of very low-concentration metabolites and similarly for the case that precision is to be optimized in order to detect very small changes in the concentration of standard brain metabolites (e.g. in longitudinal clinical exams). The exploration yielded results in terms of optimal VS for single voxel examinations and fitting conditions in 3T brain scans, where target results are not linked to a certain brain location or gray / white matter proportion.

Optimal voxel size

Considering CRLB as the overall indicator of quantification precision, it turned out that increasing the VS up to roughly 70 cm^3 is advisable independent of the fitting method. For larger VS there is no or only small further gain in terms of CRLB and linewidth while artifact burden may increase substantially in some cases, e.g. when the voxel is placed close to the skull.

We have demonstrated the VS dependence of metabolite CRLBs by figures for metabolites that have large concentrations and thus are well represented in the spectra. It should be stressed, however, that the absolute CRLBs behave similarly for strong and weakly represented metabolites since they are mainly determined by the mutual overlap of peak patterns. Supplemental Figure S3 contains data for some low-concentration metabolites that show the same VS dependence. In addition, it may be useful to mention that the absolute CRLBs for the presented metabolites correlate strongly for measurements at different voxel sizes with the squared correlation coefficients >>0.99 independent of the concentration of the metabolites involved. Hence, the recommendation for optimal VS is independent of the type of metabolite.

Comparing Figure 2 and Figure 4 suggests that the ideal VS depends somewhat on the way the spectra are fitted. Even though that is true, we would not recommend to go > 75 cm^3 VS in a routine fashion also when using simultaneous fitting from multiple coil elements because of the reduced robustness for very large VS (i.e. appearance of spurious outer volume signals at very large VS – in particular subsequent to small subject motion) – at least if not combined with automated motion correction methods.

Differences between coil elements

Inspection of the signals acquired by the individual coil elements revealed significant differences in the signals recorded from different spatial viewpoints relative to the ROI. As expected, signal

intensity differs substantially between the channels also for very large VS. However, the routinely implemented summation over coil elements includes intensity-weighted averaging, such that this issue is already taken care of in the standard coil averaging routine. Less expectedly, center frequency offset shifts between the coil elements were also found. Furthermore, the reference water measurements registered by the individual coils revealed substantial differences in overall lineshape (c.f. Figure 3), offering another reason to evaluate individual coil spectra with their respective lineshapes. In addition, appearance of outer-volume lipid artifacts proved to depend on the position of the coil. This is especially plausible for large voxels, which have to be positioned close to the skull, and where this easily leads to excitation of outer-volume lipid signals - either caused by imperfect ROI profiles or chemical shift artifacts that shift the ROI for 1.3 ppm resonances very close to or within subcutaneous fat.

Differences between the individual coil channels proved to be surprisingly large, not only in terms of signal intensity, but also regarding overall spectral quality, such as linewidth, lineshape or appearance of artifacts but also frequency shifts. As the ROIs used in this study were relatively large, the different channels recorded spatially-weighted signals from substantially different regions of the ROI. This leads to differences in signal composition and B_0 homogeneity, reflected in the lineshape. Also, the intensity of artifacts, in particular spurious lipid signals, highly depends on the region in the location of the coil element with respect to the place of origin of the artifact.

Postprocessing and fitting

Confirming earlier results[16,32], use of the lineshape information from the reference water signal helped improve the fit precision in general, especially when it comes to poor overall shim performance. A simultaneous fit of the channels was evaluated as an alternative to the traditional way of fitting the weighted sum spectrum. Using the reference lineshape for each coil, the frequency shifts and distortions of the lineshape were accounted for individually. In FiTAID, a combined fit of inter-related datasets is possible, such that an overall quantification of the metabolites can be performed easily. The differences in signal intensity between channels are taken into account automatically by the reference signals multiplied into the model. Lower CRLB showed that this method is superior to fitting the weighted sum, especially when it comes to large VS and even more so with poor shim performance. For the optimal VS, a reduction in CRLB of approximately 10% can be expected with this method.

Another aspect that motivates close inspection of data from individual coil elements is the difference in artifacts. This issue is particularly relevant in case of very large VS, where prominent lipid peaks can be expected. We investigated excluding channels with large artifacts from the overall sum. An automated method was tested to find spectra that show significant differences from the expected shape. Normalization of the spectra to their maximum metabolite signal was found to help the comparison of all channels despite their differences in SNR. However, the improvement of spectral quality from the automated method for spectra with significant artifacts was very small in most cases. For the PRESS data, however, a clear improvement of the spectral quality could be visually judged with no loss in SNR, showing that the proposed method is promising for non-ideal experimental settings. However, one should also keep in mind whether the remaining outer-volume signals are really tolerable. Furthermore, the exclusion of certain coil elements may influence the composition of the voxel, e.g. regarding effective volume distribution of grey and white matter that might not be taken meaningfully any more from simple segmentation.

In this context, it may be worthwhile to return to the idea of post-acquisition summation (or simultaneous fitting) of spectra from an arbitrary region in a CSI scan. As mentioned above, this would not be optimal in terms of SNR, but may eliminate certain outer-volume signals and in a simultaneous fitting approach with enforced reference lineshapes still provide enough effective SNR for precisions that come close to those of the presently shown “brute-force” single voxel approach. Of course also in a CSI scan individual coil elements could be evaluated separately to further reduce artifacts.

Limitations

In this study, the differences in tissue compositions for different VS have not been considered. Spectra were normalized with the water signal, but overall water content may differ for different VS. However, we do not expect that including water content into our calibrations would alter any of the main conclusions.

A further aspect of differing voxel composition is relevant in terms of applications. The mixed voxel content is not a problem in individual follow-up studies where small metabolite changes may trigger a change in treatment. In such a case of watchful waiting, of course MRI assays of compartment volumes would be included in the investigations. However for cohort studies, care should certainly be used to guarantee that potential group differences are not related to gray/white matter disparities.

Because there is no ground truth information in terms of brain metabolite content for individual subjects, CRLB, i.e. a measure for fitting precision, was used as optimization criterion as a proxy for

the accuracy of the determined metabolite content. In follow-up, it would be advisable to look into repeatability of results from the proposed large VS and advanced modeling vs. more standard acquisition conditions. In addition, it would also be of interest to investigate whether weighted averaging using other than SNR-weighting could outweigh the proposed benefit of simultaneous fitting of individual coil elements and whether such approaches can be combined.

The choice of ROI in this study in terms of shape, direction and brain region gave optimal conditions for shimming performance and therefore encouraged the use of very large VS. Missetting the shimming parameters simulates a less optimal condition, but does not mimic all difficulties which might appear when e.g. a different brain region is chosen. Also, the impact of missetting the shim increases with VS, which has to be considered when comparing VS for the misset shim cases.

In this study we used the relatively high concentrated metabolites Cr, mI and Glu for evaluation of the CRLB. In a clinical investigation of global brain pathology, metabolites with a much lower concentration such as NAD^+ or Phenylalanine would be of interest, as stated earlier. As these metabolites resonate at the downfield part of the spectrum, an evaluation of CRLB of a metabolite from this frequency range would be of interest. However, as there is no sufficient knowledge on the metabolite responses at the downfield region yet, the simulation of a realistic model is not possible. Further studies will be necessary to prove that the results from the high concentrated upfield metabolites are transferable to the proposed applications.

As no exact metabolite response simulations for the used semi-LASER sequence were available at the time, simulations from an ideal PRESS sequence were used for the fitting model. The heuristic method of finding the best matching TE in PRESS for the semi-LASER sequence suggested in[30] was used. We expect that the influence of a slight mismatch between simulated and in vivo spectral patterns is negligible for the findings of this paper because the calculation of CRLBs for different VS (depending on the partial derivates with respect to frequency and linewidth) will not be systematically different for base spectra with similar shape).

Generalization of the recommendations

It should also be noted that the recommendations for VS and post-processing are explicitly only valid for the given settings in this study, especially with regard to field strength (3T), the shimming methods and the localization sequence used. Furthermore, as the spectra in this study were recorded with a semi-LASER sequence with partial outer volume suppression, the setting for use of a large VS was optimal. For a different sequence, like standard PRESS, the spectral quality with such a large VS is expected to be lower due to the considerably larger chemical shift artifact (see Fig. 5).

5. Conclusion

Optimal VS for the use of MRS in non-focal disease was evaluated as a compromise between SNR and metabolite linewidth as well as artifact appearance, showing that a ROI size up to 70 cm^3 is beneficial in terms of quantification precision. Including the lineshape information of a water reference measurement can improve the fitting performance, especially for B_0 inhomogeneity caused by poor shimming. In addition, the signals recorded by the individual coil elements showed severe differences in spectral quality such that it turned out to be useful to simultaneously fit these individual channel spectra with enforced lineshape and coil sensitivity information rather than combining the signals with subsequent fitting.

Acknowledgement

This work was supported by the Swiss National Science Foundation (320030-156952 and 320030-175984).

The semi-LASER sequence was developed by Edward J. Auerbach and Malgorzata Marjańska and kindly provided by the University of Minnesota under a C2P agreement.

References

1. Kreis R. 1H-magnetic resonance spectroscopy of cerebral phenylalanine content and its transport at the blood-brain barrier. In: *Neural Metabolism In Vivo, edited by I. Y. Choi and R. Gruetter. New York: Springer*; 2012:1117–1134.
2. de Graaf RA, De Feyter HM, Brown PB, Nixon TW, Rothman DL, Behar KL. Detection of cerebral NAD^+ in humans at 7T. *Magn Reson Med*. 2017;78(3):828–835. doi:10.1002/mrm.26465
3. Fleysher R, Fleysher L, Liu S, Gonen O. On the voxel size and magnetic field strength dependence of spectral resolution in MR spectroscopy. *Magn Reson Med*. 2009;27(2):222–232. doi:10.1016/j.mri.2008.06.009
4. Bartha R. Effect of signal-to-noise ratio and spectral linewidth on metabolite quantification at 4 T. *NMR Biomed*. 2007;20(4):512–521. doi:DOI:10.1002/nbm.1122
5. Juchem C, de Graaf RA. B_0 magnetic field homogeneity and shimming for in vivo magnetic resonance spectroscopy. *Anal Biochem*. 2017;529:17–29. doi:10.1016/j.ab.2016.06.003
6. Hanson LG, Adalsteinsson E, Pfefferbaum A, Spielman DM. Optimal voxel size for measuring global gray and white matter proton metabolite concentrations using chemical shift imaging. *Magn Reson Med*. 2000;44:10–18.
7. Cavassila S, Deval S, Huegen C, Van Ormondt D, Graveron-Demilly D. Cramér-Rao bounds: An evaluation tool for quantitation. *NMR Biomed*. 2001;14(4):278–283. doi:10.1002/nbm.701
8. Bolliger CS, Boesch C, Kreis R. On the use of Cramér-Rao minimum variance bounds for the design of magnetic resonance spectroscopy experiments. *Neuroimage*. 2013;83:1031–1040. doi:10.1016/j.neuroimage.2013.07.062
9. Provencher SW. Estimation of metabolite concentrations from localized in vivo proton NMR spectra. *Magn Reson Med*. 1993;30:672–679.
10. Slotboom J, Boesch C, Kreis R. Versatile frequency domain fitting using time domain models and prior knowledge. *Magn Reson Med*. 1998;39:899–911.
11. Kreis R, Slotboom J, Hofmann L, Boesch C. Integrated data acquisition and processing to determine metabolite contents, relaxation times, and macromolecule baseline in single examinations of individual subjects. *Magn Reson Med*. 2005;54(4):761–768. doi:10.1002/mrm.20673
12. Klose U. In vivo proton spectroscopy in presence of eddy currents. *Magn Reson Med*. 1990;14:26–30.
13. de Graaf A, van Dijk J, Bovée W. QUALITY : Quantification improvement by converting lineshapes to the lorentzian type. *Magn Reson Med*. 1990;13:343–357.
14. Barker PB, Soher BJ, Blackband SJ, Chatham JC, Mathews VP, Bryan RN. Quantitation of proton NMR spectra of the human brain using tissue water as an internal concentration reference. *NMR Biomed*. 1993;6(1):89–94.
15. Bartha R, Drost DJ, Menon RS, Williamson PC. Spectroscopic lineshape correction by QUECC: Combined QUALITY deconvolution and eddy current correction. *Magn Reson Med*. 2000;44(4):641–645.
16. Adalid V, Döring A, Kyathanahally SP, Bolliger CS, Boesch C, Kreis R. Fitting interrelated datasets: metabolite diffusion and general lineshapes. *MAGMA*. 2017;30(5):429–448.
17. Dydak U, Weiger M, Pruessmann KP, Meier D, Boesiger P. Sensitivity-encoded spectroscopic imaging.

Magn Reson Med. 2001;46:713–722.

18. Brown MA. Time-domain combination of MR spectroscopy data acquired using phased-array coils. *Magn Reson Med*. 2004;52(5):1207–1213. doi:10.1002/mrm.20244
19. Natt O, Bezkorovaynyy V, Michaelis T, Frahm J. Use of phased array coils for a determination of absolute metabolite concentrations. *Magn Reson Med*. 2005;53(1):3–8. doi:10.1002/mrm.20337
20. Maril N, Lenkinski RE. An automated algorithm for combining multivoxel MRS data acquired with phased-array coils. *J Magn Reson Imaging*. 2005;21(3):317–322. doi:10.1002/jmri.20261
21. Bydder M, Hamilton G, Yokoo T, Sirlin CB. Optimal phased-array combination for spectroscopy. *Magn Reson Imaging*. 2008;26(6):847–850. doi:10.1016/j.mri.2008.01.050
22. Dong Z, Peterson B. The rapid and automatic combination of proton MRSI data using multi-channel coils without water suppression. *Magn Reson Imaging*. 2007;25(8):1148–1154. doi:10.1016/j.mri.2007.01.005
23. Hall EL, Stephenson MC, Price D, Morris PG. Methodology for improved detection of low concentration metabolites in MRS: Optimised combination of signals from multi-element coil arrays. *Neuroimage*. 2014;86:35–42. doi:10.1016/j.neuroimage.2013.04.077
24. Wu M, Fang L, Ray CE, Kumar A, Yang S. Adaptively optimized combination (AOC) of phased-array MR spectroscopy data in the presence of correlated noise: Compared with noise-decorrelated or whitened methods. *Magn Reson Med*. 2017;78(3):848–859. doi:10.1002/mrm.26504
25. Slotboom J, Nirkko A, Brekenfeld C, Van Ormondt D. Reliability testing of in vivo magnetic resonance spectroscopy (MRS) signals and signal artifact reduction by order statistic filtering. *Meas Sci Technol*. 2009;20:104030. doi: 10.1088/0957-0233/20/10/104030
26. Marjanska M, Auerbach E. Spectroscopy package. *https://www.cmrr.umn.edu/spectro/*.
27. Chong DGQ, Kreis R, Bolliger CS, Boesch C, Slotboom J. Two-dimensional linear-combination model fitting of magnetic resonance spectra to define the macromolecule baseline using FiTAID, a Fitting Tool for Arrays of Interrelated Datasets. *MAGMA*. 2011;24(3):147–164. doi:10.1007/s10334-011-0246-y
28. Stefan D, Di Cesare F, Andrasescu A, et al. Quantitation of magnetic resonance spectroscopy signals: The jMRUI software package. *Meas Sci Technol*. 2009;20:104035. doi:10.1088/0957-0233/20/10/104035. doi:10.1088/0957-0233/20/10/104035
29. Soher BJ, Semanchuk P, Todd D, Steinberg J, Young K. VeSPA: Integrated applications for RF pulse design, spectral simulation and MRS data analysis. In: *Proceedings of the 19th Annual Meeting of ISMRM, Montreal, Canada, 2011. p. 1410*.
30. Boer V, van Lier A, Hoogduin J, Wijnen J, Luijten P, Klomp D. 7T 1H MRS with adiabatic refocusing at short TE using radiofrequency focusing with a dual-channel volume transmit coil. *NMR Biomed*. 2011;24(9):1038–1046.
31. Cao P, Wu EX. In vivo diffusion MRS investigation of non- water molecules in biological tissues. *NMR Biomed*. 2016:e3481. doi: 10.1002/nbm.3481. doi:10.1002/nbm.3481
32. Li N, An L, Shen J, Branch MI. Spectral fitting using basis set modified by measured B0 field distribution. *NMR Biomed*. 2015;28(12):1707–1715. doi:10.1002/nbm.3430

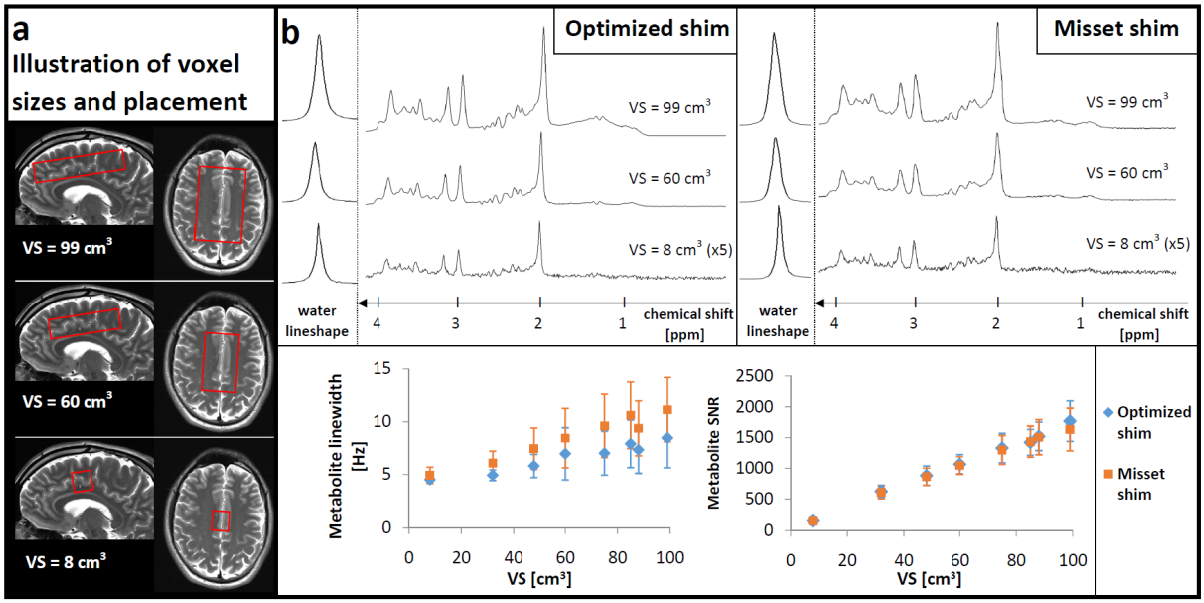

Figure 1 – *a: Illustration of voxel size and placement for three ROIs. b: Dependence of SNR and linewidth on VS for optimized and misset shim. Above: Representative spectra for the three sizes, illustrating the changes in SNR and linewidth; Below: SNR and metabolite linewidth evaluated for all subjects. SNR increases linearly with VS. Linewidth increases as well though in a non-linear fashion and with a clear difference between the optimized and misset shim cases.*

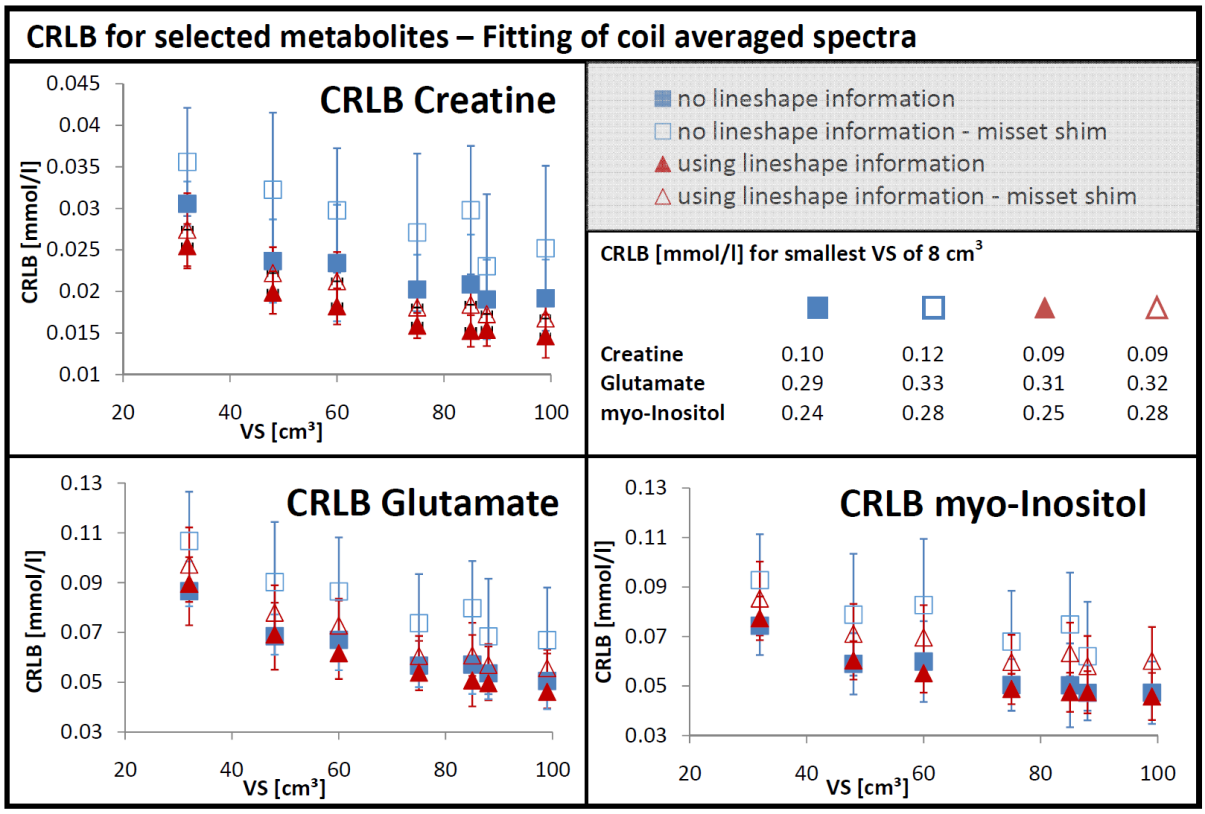

Figure 2 - *CRLB depicted as function of VS for three representative metabolites: CRLB clearly decrease up to a VS of around 75 cm³; beyond, there is only a marginal benefit for some metabolites. Using lineshape information reduces CRLB, especially for larger linewidths caused by misset shims; CRLB for the smallest VS of 8 cm³ (values included in tabulated form) showed values 2–3 times higher than the next VS of 32 cm³.*

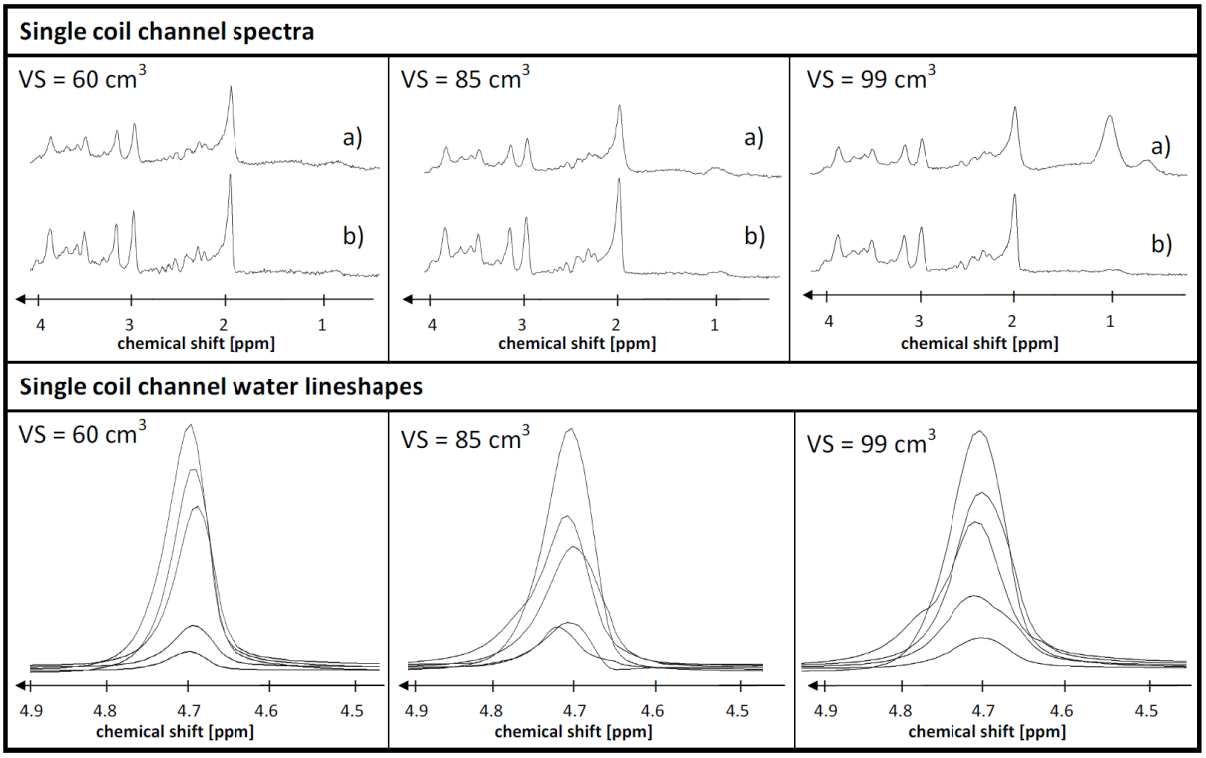

Figure 3 - *Differences between individual coil elements. Above: Representative spectra for three different, relatively large VS showing differences in spectral resolution and artifact appearance for two coil channels each with comparable signal intensity; a) a channel with large lipid artifact and low spectral resolution and b) a coil element with small lipid artifact and high spectral resolution. Below: representative water lineshapes for the three VS, showing differences in signal intensity, frequency offset and lineshape. Spectra from optimal shim settings are presented. Intensity is scaled individually for each VS for better visualization.*

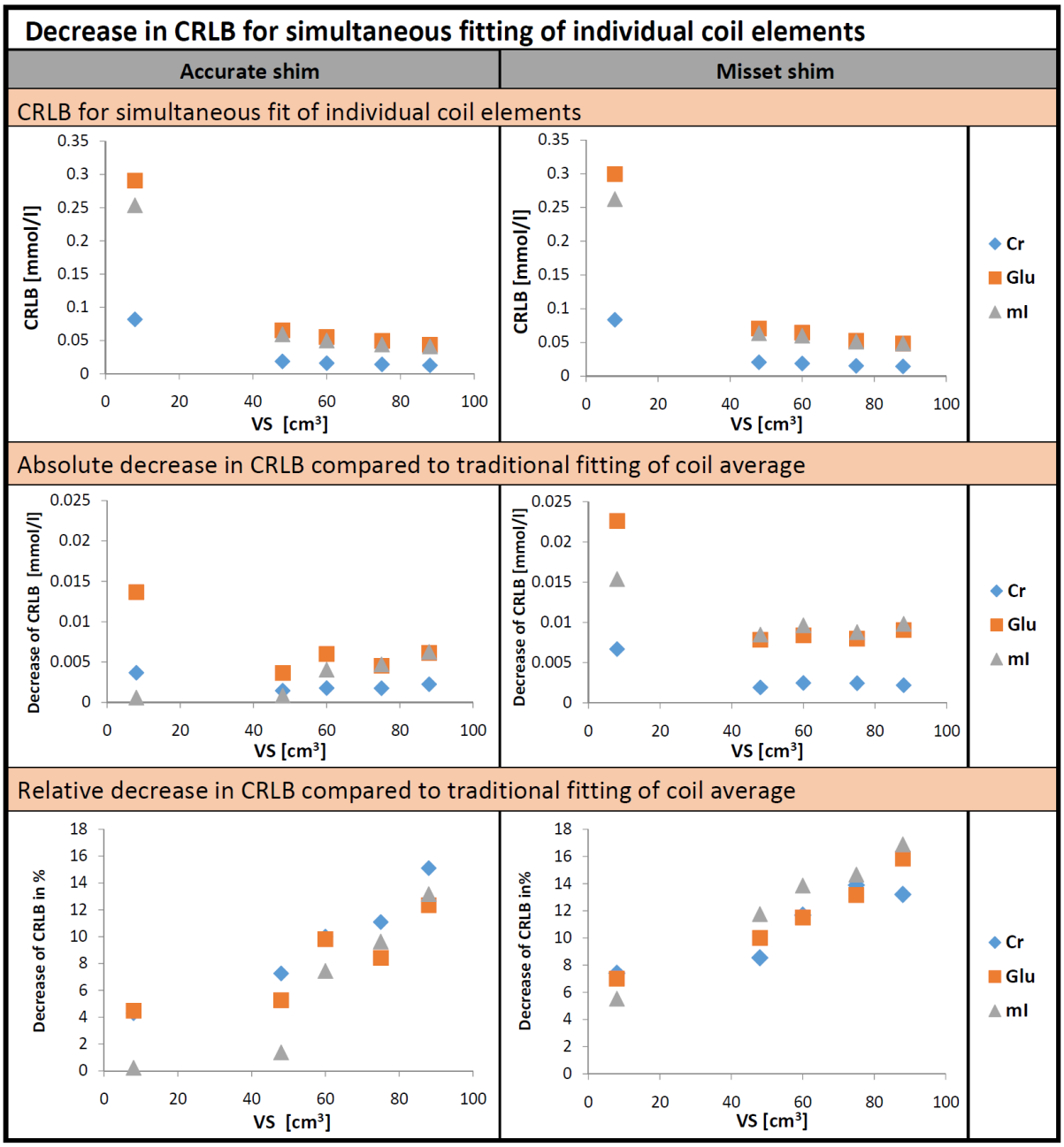

Figure 4 - *CRLB for simultaneous fitting of the individual coil element spectra and their decrease compared to fitting the averaged spectrum with lineshape information. Absolute CRLB for the 5 evaluated VS is given in the top row, the absolute decrease is pictured in the middle and the relative decrease at the bottom. Fitting the individual coil elements simultaneously reduced the CRLB in all cases for the chosen three representative metabolites. The degree of decrease depends on shim performance and VS.*

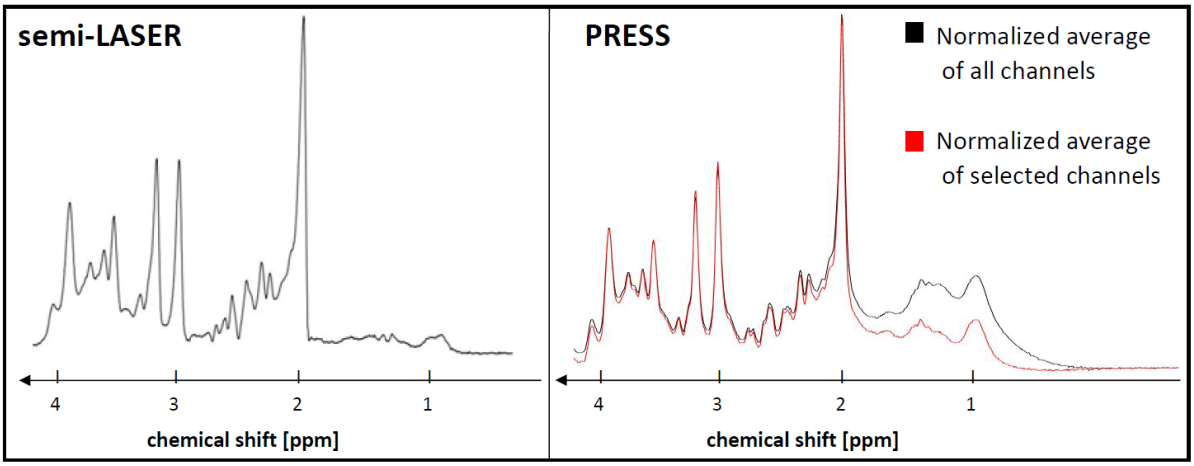

Figure 5 - *Comparison of spectra recorded from a large voxel (55x80x20 mm^3) with either semi-LASER (as for the rest of the study) or the manufacturer's PRESS sequence (TE 30 ms, TR 3000 ms, 32 acquisitions, no outer volume suppression, spectra scaled for equal intensity of NAA peak). It is apparent that PRESS in this configuration is less suitable for such a large ROI, but also that automatic exclusion of individual coil channels is more relevant in cases with stronger contamination with outer volume signals. (Bandwidths of the used refocusing pulses are largely different with the hyperbolic secant pulses used (8 ms length) in semi-LASER providing 2.4 kHz and the Mao pulses in PRESS at 1150 Hz in this exam (exact pulse length and thus bandwidth depend on the type of RF coil and its loading condition).*

Supplements

S1. Detection and quantification of artifacts resulting in exclusion of coil elements

For the exclusion of those channels that show large artifacts, an automated detection scheme for such spectra was developed. The procedure described in the following was implemented in MATLAB. As SNR differs over the individual coil elements and weighted averaging according to SNR is used, it is necessary to evaluate the artifact size relative to the signal intensity rather than its absolute size. As the purpose of this process was mainly to find artifacts caused by broad lipid signals, a range of 5 adjacent points (average over 4.9 Hz) was considered instead of single spectral points. In this compressed spectrum, the NAA peak at 2 ppm, representing the most prominent peak in the region of interest, was detected and all channels were normalized to this maximal value. Subsequently the median spectrum from all coil elements was calculated. Next, those channels were rejected where the spectrum extended outside a band around the median spectrum (threshold can be varied individually, regarding on how strict the rejection criterion should be; here it was defined by ±22.5% of the maximal signal value) anywhere in the spectral range of interest of 0–4 ppm. As the problem of severe outer volume signal artifacts is more relevant for large voxel size the scheme was tested for a size of 88 cm^3 for optimized and misset shim in all subjects.

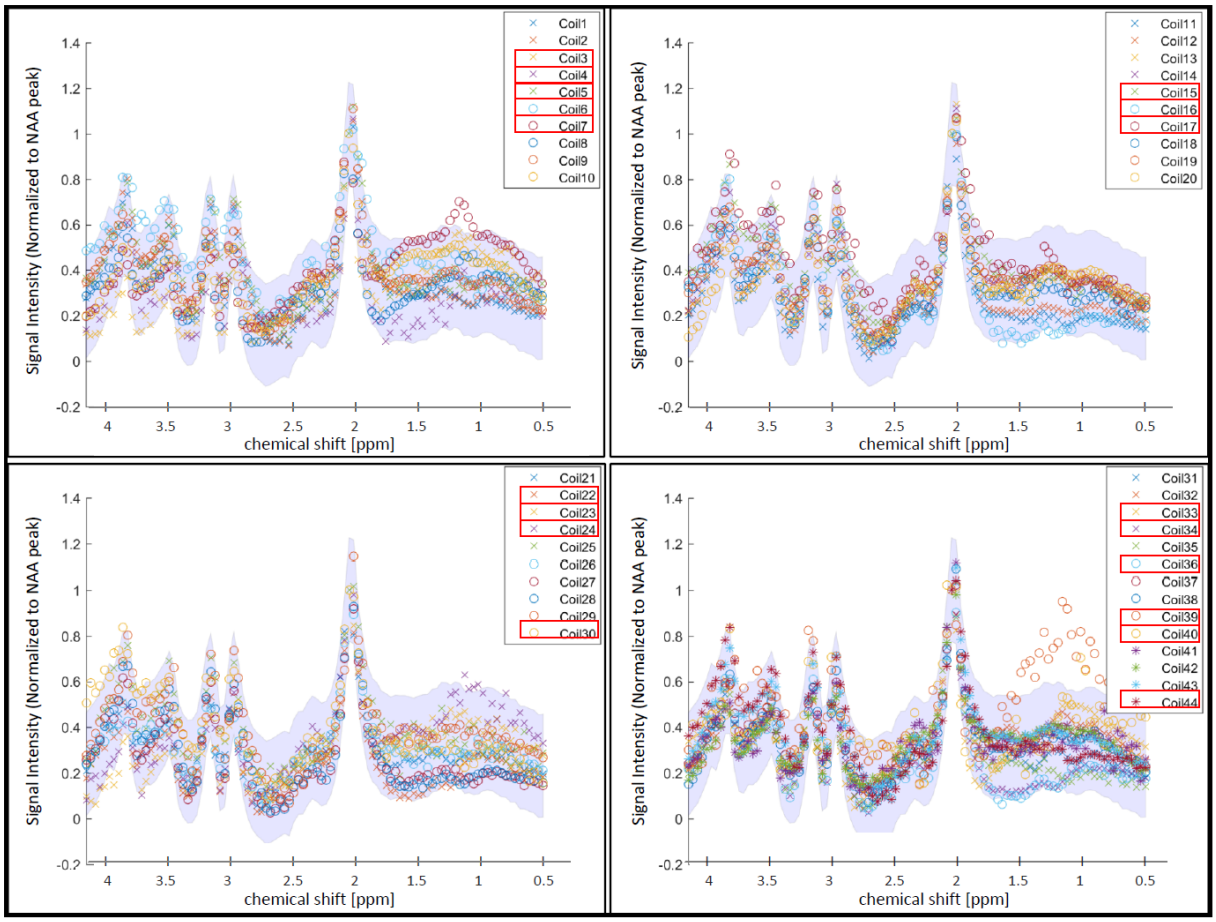

Figure S1 - *Visualization of artifact detection for a representative spectrum with a voxel size of 88 cm^3 and a misset shim. The decision to exclude a channel was based on the difference between the signal under consideration and the allowed area around the median spectrum (indicated in blue). Individual channels are identified by symbol and color. Those channels that were excluded due to exceeding the accepted interval at some location in the spectral area of interest are framed in red.*

S2. Simulation of metabolite responses

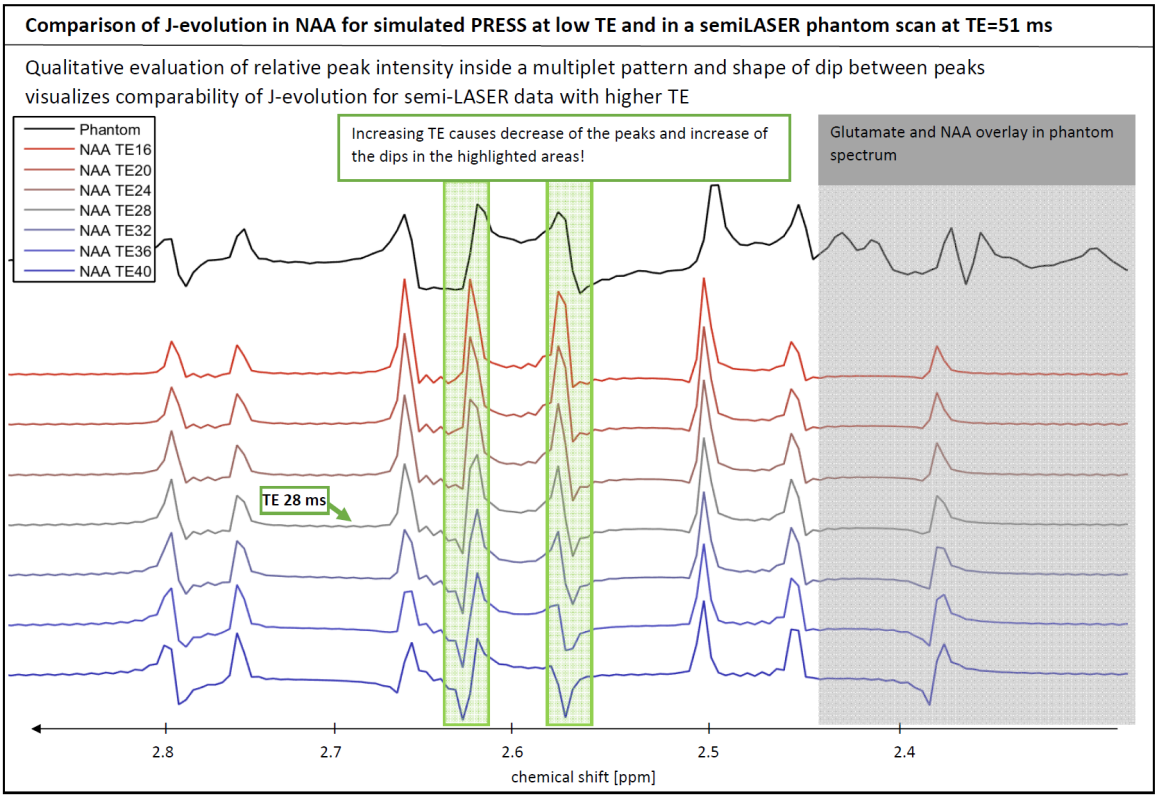

Figure S2 – *Comparison of PRESS simulated NAA response between 2.4 and 2.8 ppm for TE between 16 ms and 40 ms with in vitro scan of BRAINO phantom with semi-LASER at TE of 51 ms. J-evolution in this frequency range shows that the PRESS simulation at TE 28 ms is comparable to the semi-LASER scan at 51 ms.*

S3. CRLB for low-concentrated metabolites

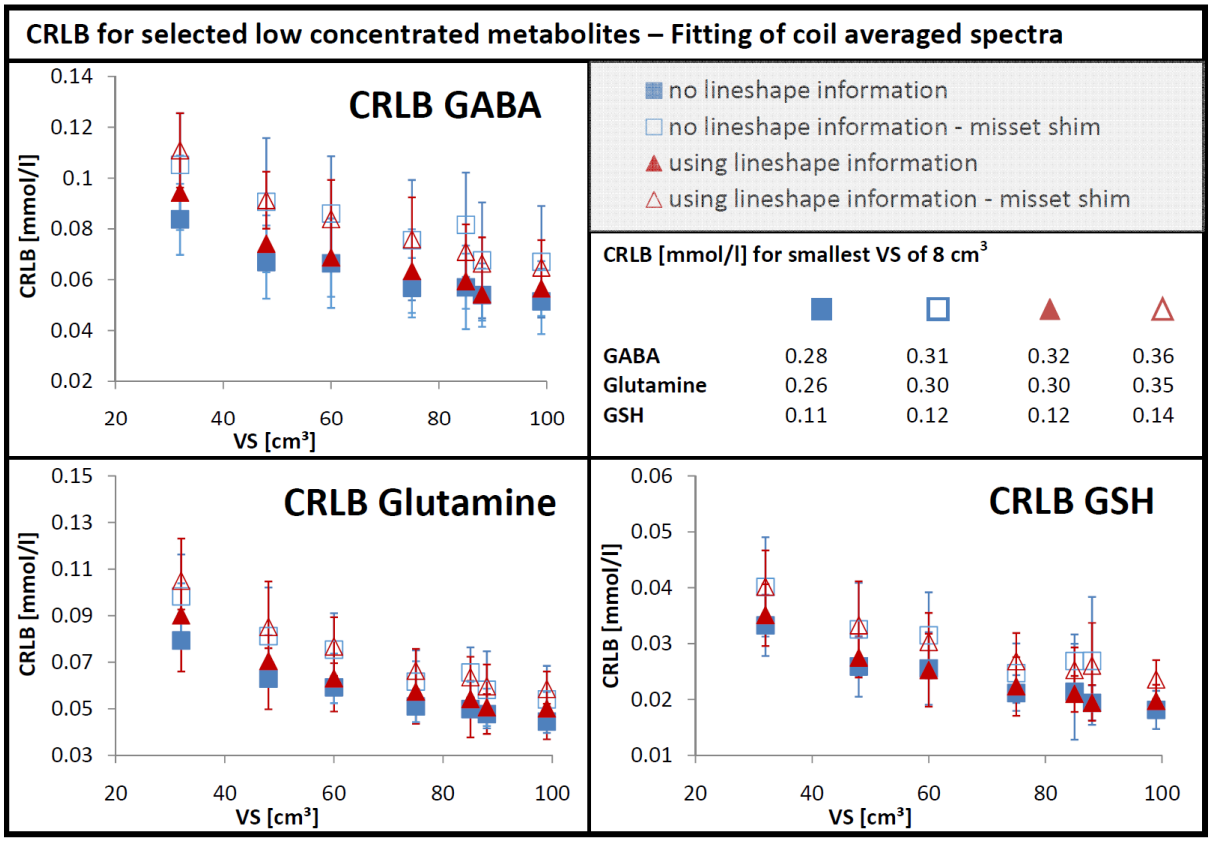

Figure S3 - *CRLB depicted as function of VS for three representative low concentrated metabolites (Gln, GSH, GABA). Comparing these to the CRLB given in Figure 2 for the high concentrated metabolites (Cr, Glu, mI) used for the VS evaluation in this study shows that the dependence of CRLB on VS is similar for all metabolites in the basis set, independent of concentration.*